Video Article

Quantifying Microorganisms at Low Concentrations Using Digital Holographic Microscopy (DHM)

Manuel Bedrossian[1], Casey Barr[2], Chris A. Lindensmith[3], Kenneth Nealson[2], Jay L. Nadeau[1]

[1]Department of Medical Engineering, California Institute of Technology

[2]Department of Earth Sciences, University of Southern California

[3]Jet Propulsion Laboratory, California Institute of Technology

Correspondence to: Jay L. Nadeau at jnadeau@caltech.edu

URL: https://www.jove.com/video/56343
DOI: doi:10.3791/56343

Keywords: Bioengineering, Issue 129, Volumetric microscopy, holographic microscopy, Mach-Zehnder, interferometric microscopy, bacterial enumeration, label-free imaging, astrobiology, life detection

Date Published: 11/1/2017

Citation: Bedrossian, M., Barr, C., Lindensmith, C.A., Nealson, K., Nadeau, J.L. Quantifying Microorganisms at Low Concentrations Using Digital Holographic Microscopy (DHM). *J. Vis. Exp.* (129), e56343, doi:10.3791/56343 (2017).

Abstract

Accurately detecting and counting sparse bacterial samples has many applications in the food, beverage, and pharmaceutical processing industries, in medical diagnostics, and for life detection by robotic missions to other planets and moons of the solar system. Currently, sparse bacterial samples are counted by culture plating or epifluorescence microscopy. Culture plates require long incubation times (days to weeks), and epifluorescence microscopy requires extensive staining and concentration of the sample. Here, we demonstrate how to use off-axis digital holographic microscopy (DHM) to enumerate bacteria in very dilute cultures (100-10^4 cells/mL). First, the construction of the custom DHM is discussed, along with detailed instructions on building a low-cost instrument. The principles of holography are discussed, and a statistical model is used to estimate how long videos should be to detect cells, based on the optical performance characteristics of the instrument and the concentration of the bacterial solution (**Table 2**). Video detection of cells at 10^5, 10^4, 10^3, and 100 cells/mL is demonstrated in real time using un-reconstructed holograms. Reconstruction of amplitude and phase images is demonstrated using an open-source software package.

Video Link

The video component of this article can be found at https://www.jove.com/video/56343/

Introduction

Determination of accurate bacterial counts in very dilute samples is crucial in many applications: a few examples are water and food quality analysis[1,2,3]; detection of pathogens in blood, cerebrospinal fluid, or sputum[4,5]; production of pharmaceutical products, including sterile water[6]; and environmental community analysis in oligotrophic environments such as the open ocean and sediments[7,8,9]. There is also increasing interest in detection of possible extant microbial life on the icy moons of Jupiter and Saturn, particularly Europa[10,11] and Enceladus[12,13,14], which are known to have subsurface liquid oceans. Because no mission since Viking in 1978 has attempted to find extant life on another planet, there has been limited development of technologies and instruments for bacterial identification and counting during space missions[15].

Traditional methods of plate count find only culturable cells, which can represent a minority of species in environmental strains, sometimes <1%[16]. Plates require days or weeks of incubation for maximum success, depending upon the strain. Epifluorescence microscopy has largely replaced plate counts as the gold standard for rapid and accurate microbial enumeration. Nucleic-acid-labeling fluorescent dyes such as 4′,6-diamidino-2-phenylindole dihydrochloride (DAPI), SYBR Green, or acridine orange that bind to nucleic acids are the typical dyes used[17,18,19], though many studies use fluorescent indicators of Gram sign[20,21,22,23,24]. Using these methods without pre-concentration steps leads to limits of detection (LoDs) of ~10^5 cells per mL. Improvements in LoD are possible using filtration. A liquid sample is vacuum-filtered onto a membrane, usually polycarbonate and ideally black to reduce background. Low-background dyes such as the DNA stains mentioned above may be applied directly to the filter[25]. For accurate counting by eye, ~10^5 cells are required per filter, which means that for samples more dilute than ~10^5 cells per mL, significant sample volumes must be collected and filtered. Laser-scanning devices have been developed in order to systematically explore all regions of the filter and thus reduce the number of cells required for counting, pushing limits of detection down to ~10^2 cells per mL[26]. However, these are not available in most laboratories, and require sophisticated hardware as well as software that permit expert confirmation that observed particles are bacteria and not debris.

For reference, adults with sepsis usually begin showing symptoms at <100 cells/mL of blood, and infants at <10 cells/mL. A blood draw from an adult takes 10 mL, and from an infant, 1 mL. PCR-based methods are inhibited by the presence of human and non-pathogenic flora DNA and by PCR-inhibiting components in the blood[27,28]. Despite a variety of emerging techniques, cultures remain the gold standard for the diagnosis of bloodstream infections, especially in more rural areas or developing nations. For detection of life on other planets, thermodynamic calculations can estimate the energy budget for life and thus the expected possible biomass. 1 - 100 cells/mL are expected to be thermodynamically

reasonable on Europa[29]. It can be readily seen from these numbers that detection of very small numbers of cells in large amounts of aqueous solution is an important unsolved problem.

In this paper, we demonstrate detection of *Serratia marcescens* and *Shewanella oneidensis* (wild-type and non-motile mutant) at concentrations of 10^5, 10^4, 10^3, and 100 cells/mL using an off-axis digital holographic microscope (DHM). The key advantage of DHM over traditional light microscopy is the simultaneous imaging of a thick sample volume at high resolution—in this implementation, the sample chamber was 0.8 mm thick. These sample chambers were constructed by the soft-lithography of polydimethylsiloxane (PDMS) from a precision-machined aluminum mold with a tolerance of ± 50 µm. This represents an approximately 100-fold improvement in depth of field over high-power light microscopy. DHM also provides quantitative phase information, allowing for measurements of optical path length (product of refractive index and thickness). DHM and similar techniques have been used for monitoring bacterial and yeast cell cycle and calculation of bacterial dry mass[30,31,32]; scattering differences may even be used to differentiate bacterial strains[33].

The instrument we use is custom-built specifically for use with microorganisms, as previously published[34,35], and its design and construction are demonstrated and discussed. Aqueous solutions are continuously supplied to a 0.25 µL volume sample chamber via syringe pump; the flow rate is determined by camera frame rate in order to ensure imaging of the entire sample volume. A statistical calculation predicts the number of sample volumes that must be imaged in order to detect a significant number of cells at a given concentration.

For cell-detection applications, reconstruction of the holograms into amplitude and phase images was not required; analysis was performed on the raw hologram. This saves significant computational resources and disk space: a 500 Mb hologram video will be 1 - 2 Tb when reconstructed. However, we do discuss reconstruction through depth of the sample to confirm that the holograms represent the desired species. An important feature of DHM is its ability to monitor both intensity and phase of the images. Organisms that are nearly transparent in intensity (such as most biological cells) appear clearly in phase. As it is a label-free technique, no dyes are used. This is an advantage for possible space flight applications, since dyes may not survive the conditions of a mission and—more importantly—cannot be assumed to work with extraterrestrial organisms, which may not use DNA or RNA for encoding. It is also an advantage for work in extreme environments such as the Arctic and Antarctic, where dyes may be difficult to bring to the remote location and may degrade upon storage. Reconstruction of images into phase and amplitude is performed using an open-source software package that we have made available on GitHub (SHAMPOO) or using ImageJ.

Protocol

1. Growth and Enumeration of Bacteria

NOTE: This is applicable to almost any bacterial strain grown in the appropriate medium[36]. In our example, we use three strains: *Serratia marcescens* as a common, easy identifiable lab strain; and a smaller, highly motile environmental strain, *Shewanella oneidensis* MR-1. To compare detection of motile vs. non-motile cells, a non-motile *Shewanella* mutant, Δ FlgM, is also used for comparison[37]. All strains are grown in lysogeny broth (LB).

1. Prepare sterile LB medium (per liter of distilled water: 10 g bacto tryptone, 5 g bacto yeast, 10 g NaCl; filter or autoclave). Prepare standard 100 mm diameter LB-agar plates (same recipe as medium plus 15 g agar per liter; autoclave (121 °C, 20 min) to sterilize and pour when cool enough to handle). Store medium and plates in refrigerator.
2. The day before the experiment seed 5 - 6 mL of "Master" culture medium from a fresh bacterial colony, using correct sterile and biosafety technique. Incubate on a shaker (120 rpm) at 30 °C for ~12 h. Incubation time will be dependent on the strain and growth rate. In our experiments, the *Shewanella* strains are incubated for 12 hours; however, *Serratia* is harvested after 8 hours, to ensure the culture will be exhibiting mid-logarithmic growth.
3. The day of the experiment, take a spectrophotometric reading (OD_{600}) of the bacterial Master culture, which is expected to be in the range of 0.6 to 0.7. It should be in the logarithmic growth phase (as determined previously). If not, subculture 100 µL into 5 mL of medium and allow cell growth to the mid-log phase.
4. **Take a sample of the Master culture and count the cells directly using a Petroff-Hausser counting chamber. This will enumerate both live and dead cells.**
    1. Extract a 10 µL sample of the undiluted culture with a micropipette and transfer into the chamber.
    2. Image under a high-dry objective microscope (40X or 63X, NA 0.7 - 0.8) using phase contrast.
    3. Count the bacteria in at least 20 squares and average.
    NOTE: Count only those bacteria which are entirely within a square and only those crossing over the top and left boundaries (or bottom and right, if you prefer). If squares are separated by several lines, choose one as a boundary.
    4. Calculate concentration as the average of 20 squares x dilution factor. Note that direct counts do not work well for concentrations $<10^7$/mL.
5. **Make serial dilutions of the culture for counting of colony-forming units (CFU). This will enumerate live cells only.**
    1. Make a serial dilution of each of the selected bacterial samples with sterile 0.9% saline solution. Transfer 20 µL of the bacterial solution and dilute it with 180 µL saline. Repeat until the lowest concentration is ~10^3 cells/mL.
    2. Take 100 µL from at least two dilutions-suggested are 10^3 and 10^4/mL — and plate on an appropriate solid media plate. Spread with a sterile spreader. Perform at least 3 replicates of each dilution.
    3. Incubate at an appropriate temperature for your bacteria overnight or until colonies grow.
    4. Count colonies and calculate colony forming units (CFU) according to (# of colonies x dilution factor)/volume plated = CFU/mL. Average CFU over the replicates.

2. Preparation of Highly Dilute Samples for DHM

1. **Make serial dilutions of the Master culture for DHM and post-DHM counting of colony-forming units on LB media plates (See 1.4.1 - 1.4.4). Perform this double-blind so that the person doing the recordings is unaware of the concentration in each measured sample.**
    1. Dilute the bacteria into 10 - 15 mL of a minimal medium that will encourage motility (as appropriate) but inhibit cell division, so that the concentration of cells does not change appreciably during the experiment. This may be 0.9% saline or a more specific motility medium. For example, if using *Escherichia coli*, motility medium must contain EDTA[38]. For these examples, we use 0.9% saline.

3. Recording DHM Videos

1. Using a sterile syringe, pull in about 10 mL of the dilution of interest.
2. Connect the syringe to the DHM sample chamber using sterile fittings and tubing.
   NOTE: A custom-made microfluidic chamber was constructed in order to allow the consistent flow of sample through the optical path of the instrument. See the **Results** section for more details. Prior to the experiment, all components of the sample chamber should be sterilized by autoclaving.
3. Flow the sample from the syringe through the sample chamber continuously using a syringe pump.
   NOTE: Appropriate flow rates vary depending on fluidic channel dimensions, desired throughput as well as data acquisition limitations.
4. As the sample is flowed through the sample chamber, acquire holograms consecutively at an appropriate frame rate. A time-stamp file will be created which logs the time of each image capture to be used later during data analysis (protocol section 4). Obtain all holograms at ambient temperature (23° C). Record holograms by executing a pre-written C++ executable file provided by the camera manufacturer.
   NOTE: Appropriate frame rates vary depending on the flow rate chosen. For this experiment, it is recommended to use a frame rate such that a bacterium would be imaged >2 times as it traveled across the instrument's field of view.
5. Allow sufficient time for the entire 10 mL of sample to be flowed through the DHM.
6. To ensure that bacteria are not growing or dying during the experiments, inoculate enriched media plates with 100 µL of the spent media post-DHM image capture. Spread with a sterile spreader and incubate at appropriate temp for 24 hours; count colonies present.

4. Calculation of Cell Density and Limits of Detection

1. **With the acquired hologram videos, analyze the data for presence of bacteria.**
    1. Calculate the median pixel value for a time series of holograms then subtract this median value from each respective pixel to eliminate stationary artifacts in the hologram. This may be done in ImageJ by performing the following steps:
        1. Convert to 32-bit (Image-Type-32 bit)
        2. Calculate the median (Image-Stack-Zproject-Median)
        3. Subtract the median from the rest of the stack (Process-ImageCalculator-Subtract)
    2. Count the number of visible Airy rings and in-focus cells manually. In ImageJ, this is done by pointing at the objects with the Point tool.
    3. Each series of holograms will be accompanied by a time-stamp file (recorded at time of hologram acquisition). Use the time-stamp file to calculate the total amount of sample pumped at the time the image was captured.
2. Calculate the cell density by dividing the total number of cells detected by the total volume of sample imaged. Average 5 - 10 frames for accurate statistics.

5. Image Reconstruction to Amplitude and Phase

1. **Choose representative videos with 10 - 200 cells per frame. Load raw (not median-subtracted) holograms into the reconstruction software (examples: ImageJ Numerical Propagation[39]; SHAMPOO [GitHub]).**
    1. Using ImageJ, go to OD-Numerical Propagation-Numerical Diffraction.
    2. At the prompt, draw a Fourier mask to choose the real or virtual image and eliminate any sinusoidal noise features.
    3. Reconstruct amplitude and phase at appropriate z-steps by entering the reconstruction distance.
2. Median subtract the amplitude data to reduce noise as in 4.1.1.
3. Plot data as a 3D cube or projection. Go to Plugins—Volume Viewer.

Representative Results

The results should indicate the ability to detect living and dead bacteria at very low levels by DHM. The number of bacteria counted should be consistent with the results obtained using the Petroff-Hauser counting chamber and plate counts. Standard statistical methods provide information about the accuracy of the different detection methods at various bacterial concentrations.

Figure 1 shows the Petroff-Hausser counting chamber used as well as the microstructure of the counting chamber that is used in the direct enumeration of cells. **Figure 2A** shows a typical enriched culture plate that has been allowed sufficient time for *S. marcescens* to grow colonies (16 hours at room temperature). **Figure 2B** shows growth curves for all the strains used. While the exact spectrophotometer measurements vary, the relationship between OD_{600} and colony count should be linear within the reliable range of the spectrophotometer; we measured ~OD600 = 0.1 as ~10^8/mL. The direct Petroff-Hausser counts and colony counts should agree to within 10% until the cells begin to die as seen by turnover in the growth curve.

Figure 3 shows the design of the custom sample chambers. Custom microfluidic chambers were used for this experiment to allow the continuous flow of sample through the field of view of the holographic microscope. Standard microfluidic techniques and materials were used in the construction of the sample chambers. Blunt tipped stainless steel needles with male Luer-Lok fittings were inserted into the microfluidic device to provide inlet and outlet ports to the sample chamber. The microfluidic channel geometry was established by the soft lithography of polydimethylsiloxane (PDMS) using a machined aluminum master mold, which was compressed, via aluminum frames, between two optical quality glass windows. The PDMS establishes flow channel geometries as well as secures hypodermic needles, which provide fluid transport to and from the flow channels. These sample chambers use PDMS solely to establish flow channel geometry and thus contain no PDMS in the optical path of the instrument. Note that due to the optical nature of an off-axis holographic microscope, two micro-channels were molded parallel to each other in the sample chamber. This is intended to match optical path lengths between both arms of the interferometer (referred to as the 'specimen' and 'reference' arms). The reference channel should only contain sterile media, and should not be subject to flow.

Figure 4 shows a schematic and images of the digital holographic microscope in its laboratory implementation. It is operated by the software provided with the camera. **Figure 5** shows representative DHM data for bacterial enumeration and their correspondence with predicted numbers of cells per field of view. From the raw holograms, without reconstruction, it is possible to see and count the cells by median subtraction and manual tracking. This greatly reduces the computational burden compared to reconstructing all z-planes, as the raw holograms show the cells throughout the depth of the chamber. The appearance of cultures at different concentrations and their correspondence with plate count and Petroff-Hauser count are indicated. Total cell counts are determined by averaging the number of cells seen in each sample volume over the total number of volumes imaged. The limit of detection is determined by the total number of sample volumes imaged. In this experiment, we set a maximum limit on this value, with a maximum total of 10 mL of sample imaged in 0.25 µL increments (a total of 40,000 images per sample). The recordings are stopped before the maximum total volume is achieved if cells are clearly observed in each frame over a series of 20 frames. In a previous paper, we reported a formula for estimating the number of sample volumes needed to detect bacteria at a 50% confidence level at concentrations ranging from 1 - 10^5 cells/mL (**Table 1**). Based upon this estimate, an examination of all 40,000 frames should allow for detection of cells at 1/mL, though this calculation is computationally intensive.

Figure 6 shows the use of reconstruction software (Fiji)[39]. A single hologram is opened and the software "OD-Numerical Propagation-Numerical Diffraction" is run. The imaging parameters are given in the dialog box; amplitude, intensity, and phase may all be reconstructed. A single z plane may be chosen, or batch reconstructions may be used to reconstruct the entire depth.

Figure 7 shows reconstructions of amplitude and phase images at different depths in a selected sample. The Fourier mask used to generate the reconstructions is shown, along with a median-subtracted intensity image, a phase image, a maximum projection through the phase stack, and a volume projection of the intensity stack.

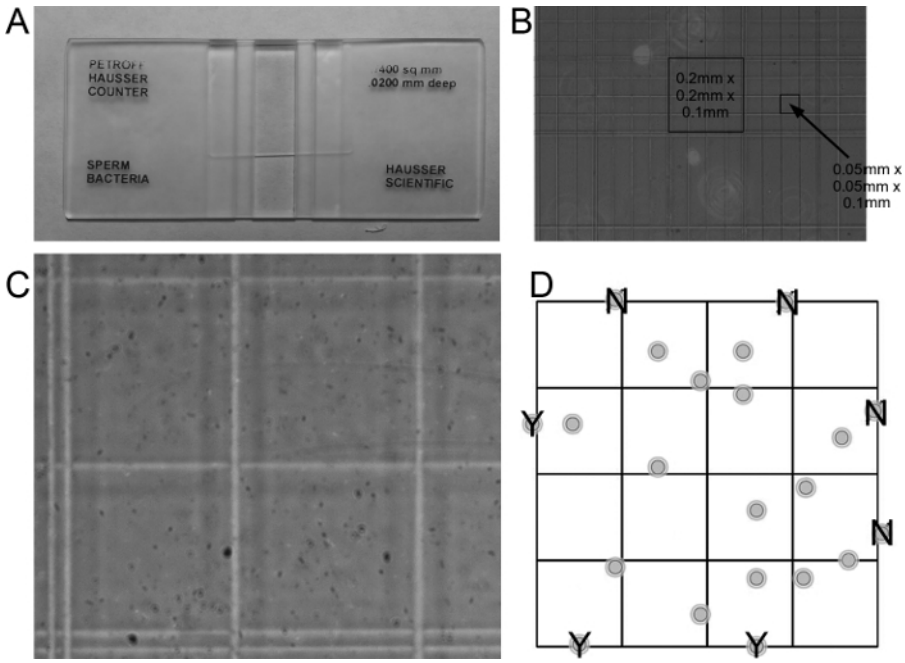

Figure 1: Direct counting of bacterial cells. Bacterial concentration in cells/mL is calculated by counting the total number of bacteria in the counting chamber and scaling that number accounting for the fact that the Petroff-Hauser chamber only contains 20 nL of sample. (**A**) The Petroff-Hausser counting chamber. (**B**) Image of counting chamber microstructure under 10X phase contrast, showing boxes of different sizes useful for enumerating cells of different sizes. (**C**) Appearance of *S. marcescens* within the counting chamber smallest boxes; 40X phase contrast. (**D**) Method for counting that excludes cells falling on the upper and right edges (N), but not the lower and left edges (Y). Please click here to view a larger version of this figure.

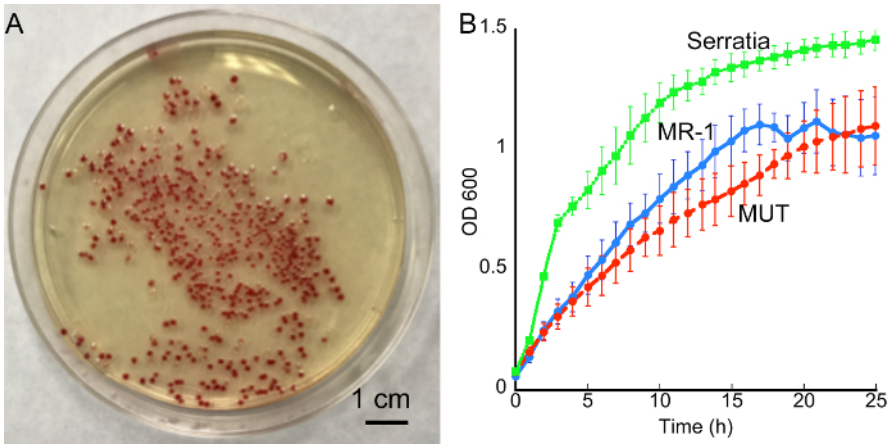

Figure 2: Counting cells by colony growth and optical density. (**A**) *S. marcescens* incubated at room temperature for 16 hours. At the correct dilution, culture plates should have 20 - 200 colonies for accurate counting and statistics. The plate shown is somewhat too crowded for reliable counting. (**B**) Growth curves for the 3 strains used. An optical density of 0.1 corresponds to ~10^8 cells/mL, but exact values vary by instrument. Direct Petroff-Hauser counts agree with plate counts to within 10% within the linear growth range. Error bars represent the standard deviation of 5 independent samples. Please click here to view a larger version of this figure.

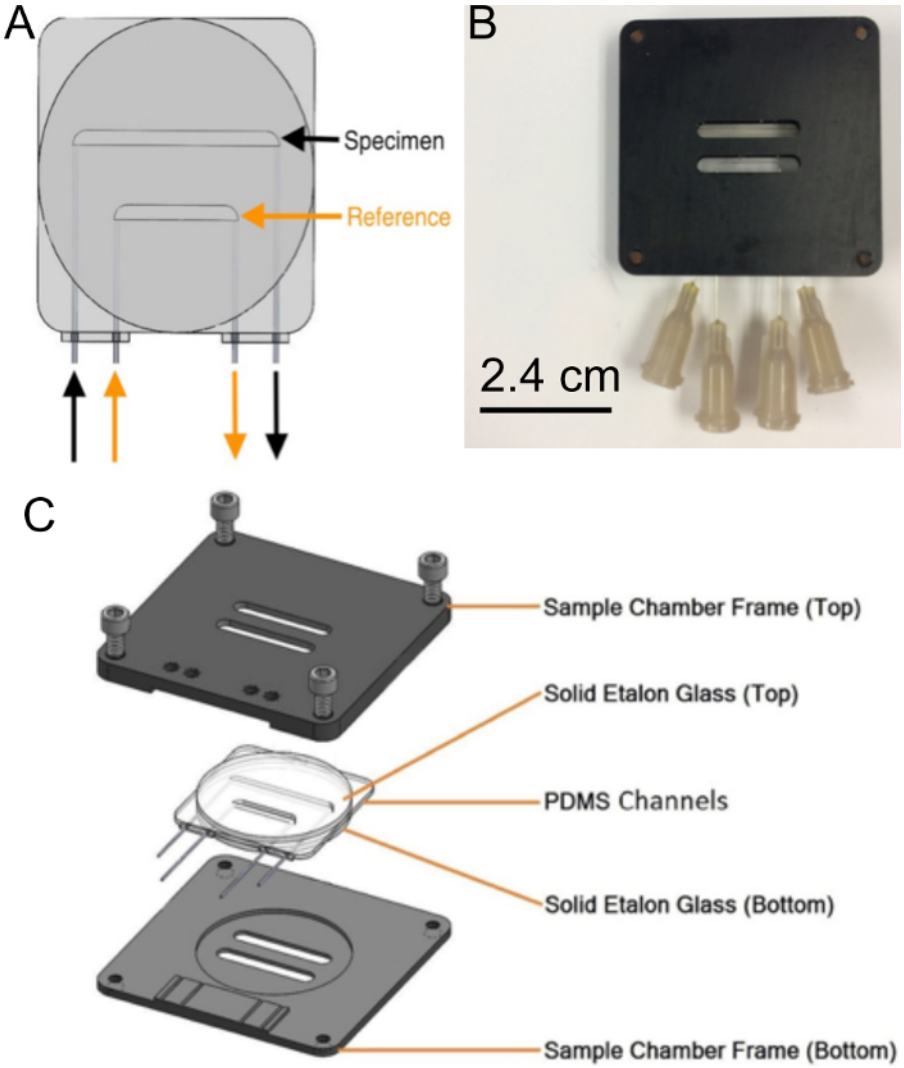

Figure 3: Sample chamber design. (**A**) Microfluidic schematic (specimen and reference microchannels labeled). (**B**) Fully assembled sample chamber. (**C**) Exploded CAD view showing the constituent elements of the sample chamber. Please click here to view a larger version of this figure.

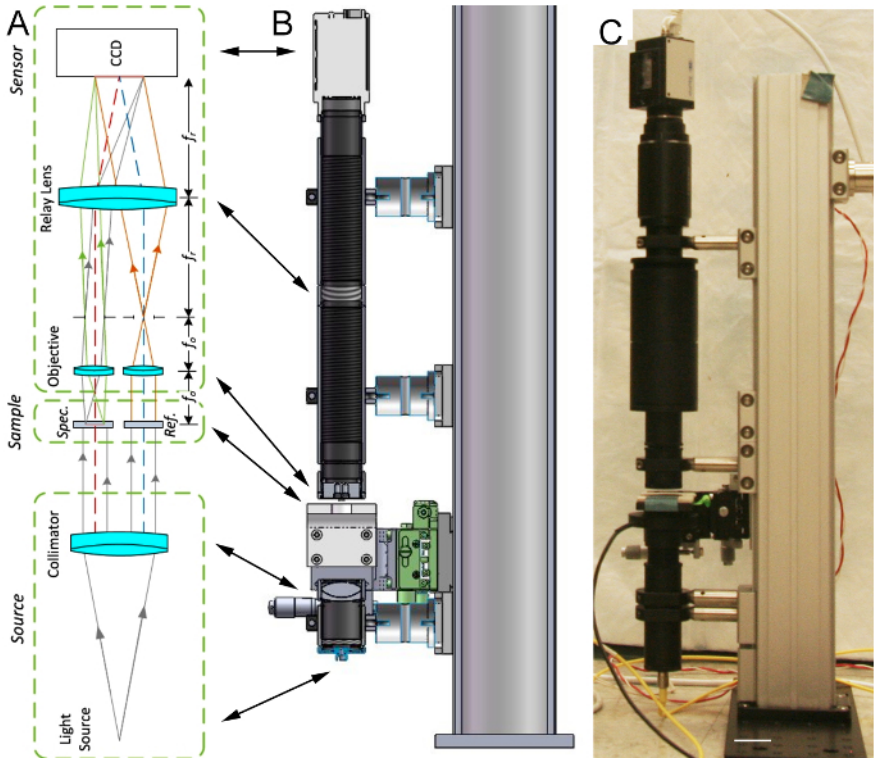

Figure 4: Schematic and images of the digital holographic microscope. (**A**) Schematic showing four main elements: the source, the sample (specimen path is labeled Spec. and reference path is labeled Ref.), the microscope, and the sensor. (**B**) Solid model of the hardware. The fiber-fed source assembly is at the bottom, and the imaging camera is at the top. The microscope optics – comprised of the two aspheric lenses and the relay lens – are contained within the 300 mm long lens tube. The three-axis stage between the source the microscope optics provides easy manual manipulation of the specimen under study. (**C**) Photograph of the instrument in the laboratory. The scale bar in the bottom portion of the image represents 1 inch. The schematics are re-drawn from Wallace *et al.*[34]. Please click here to view a larger version of this figure.

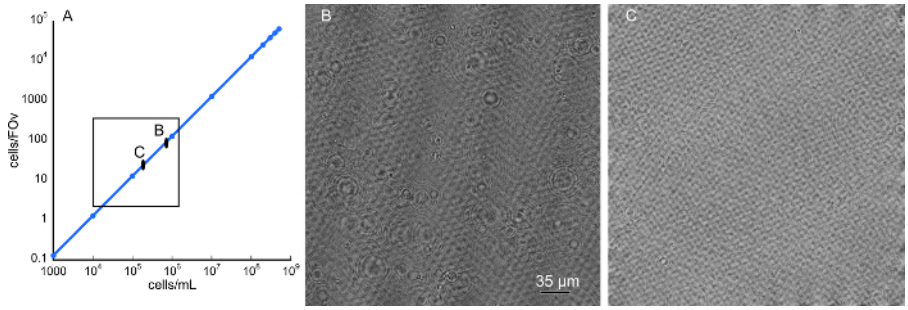

Figure 5: Growth curves and representative DHM data. (**A**) Predicted cells per field of view based upon a sample volume of 365 µm x 365 µm x 1 mm. The optimal range for DHM enumeration is shown in the rectangle, and real samples are indicated as (**B**) and (**C**). (**B**) DHM hologram of a *Shewanella* culture at 8 x 10^5 cells/mL measured by Petroff-Hauser and 7.7 x 10^5 cells/mL as measured by plate count; this image shows 110 cells, an excellent fit to the prediction. (**C**) DHM hologram of a *Shewanella* culture at 2.0 ±0.1 x 10^5 cells/mL measured by Petroff-Hauser and 2.0 ±0.3 x 10^5 cells/mL as measured by plate count; this image shows 27 cells. Scale bar = 35 µm. Please click here to view a larger version of this figure.

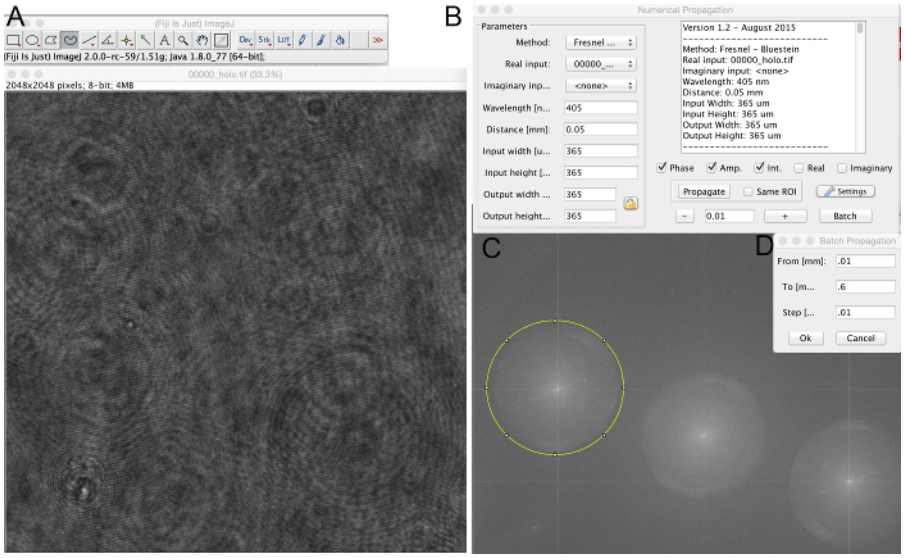

Figure 6: Performing reconstructions. (**A**) Open a hologram in Fiji. (**B**) Run Numerical Propagation and enter the wavelength and image size. Choose a z distance close to 0 to start. (**C**) Draw a Fourier mask when prompted to select the real or virtual image. (**D**) Bath processing allows for reconstructions throughout the volume. Please click here to view a larger version of this figure.

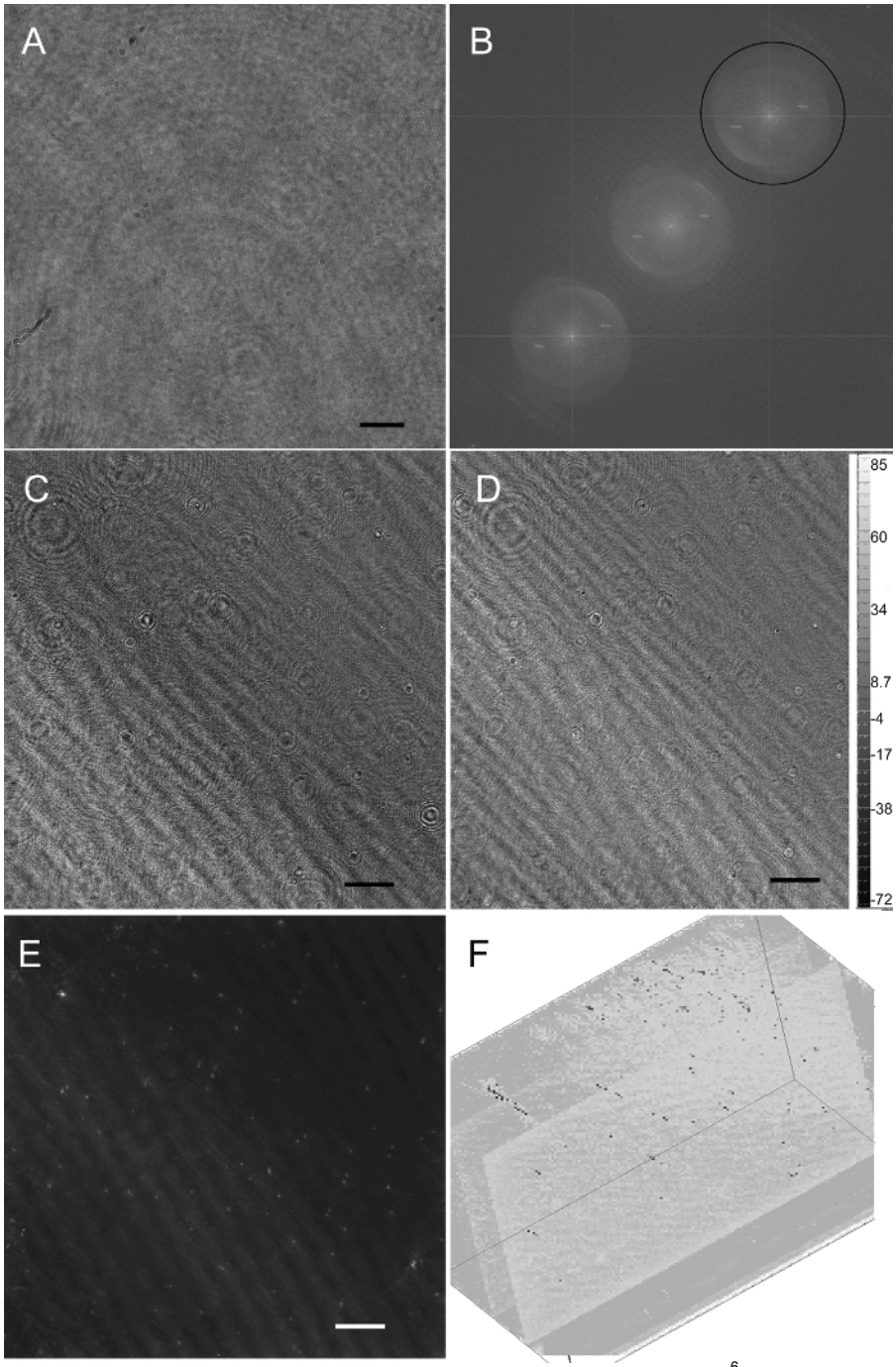

Figure 7: Appearance of reconstructions. Images of *Serratia* culture at ~10^6 cells/mL. (**A**) Raw hologram. (**B**) Fourier transform. The area inside the circle is the area to be used; the rest is masked. (**C**) Amplitude reconstruction at a single z-plane. (**D**) Phase reconstruction at a single z-plane; the scale bar shows the phase shift in degrees. (**E**) Maximum intensity projection through all z-planes in the phase stack. (**F**) Volume view of the full amplitude stack (365 x 365 x 800 µm). Scale bar = 35 µm. Please click here to view a larger version of this figure.

Concentration [cells per mL]	Frames Needed
1.00E+00	6,686
1.00E+01	669
1.00E+02	67
1.00E+03	7
1.00E+04	1
1.00E+05	1

Table 1: Minimum number of required sample volumes to detect bacteria by DHM (detection confidence of 50%).

Property	Value	Unit
Operating Wavelength	405	nm
Objective Numerical Aperture	0.3	-
System Magnification	20	-
Lateral Resolution	0.7	µm
Sample Imaging Volume	360 x 360 x 800	µm x µm x µm
Instrument Length	400	mm

Table 2: Optical and performance specifications for the digital holographic microscope.

Discussion

Numerical reconstruction of holograms: For the numerical reconstruction of holograms, the angular spectrum method (ASM) is used. This involves the convolution of the hologram with the Green's Function for the DHM. The complex wavefront of the image at a particular focal plane can be calculated by employing the Fourier Convolution Theorem as follows:

$$\Gamma(\xi,\eta) = \mathfrak{F}^{-1}(\mathfrak{F}(h(n.m)) * G(n,m)) \quad (1)$$

Where $\mathfrak{F}$ is the Fourier Transform operator, h is the hologram matrix, and G is the Green's Function of the DHM, which is defined as:

$$G(n,m) = exp\left\{\frac{-2\pi dj}{\lambda}\sqrt{1-\frac{\lambda^2\left(n+\frac{N_x^2\Delta x^2}{2d\lambda}\right)}{N_x^2\Delta x^2}-\frac{\lambda^2\left(m+\frac{N_y^2\Delta y^2}{2d\lambda}\right)}{N_y^2\Delta y^2}}\right\} \quad (2)$$

Where d is the distance, along the optical axis, of the desired focal plane to be reconstructed, λ is the illumination wavelength, N_x and N_y are the number of pixels in the x and y directions, respectively, and Δx and Δy are the pixel sizes (at the detector plane) in the x and y directions, respectively[40].

From the complex wave front, the intensity can be calculated by the magnitude squared of Γ, and the phase can be obtained by the arctangent of the quotient between the imaginary and real parts of Γ.

Modifications and troubleshooting
Experiments involving the enumeration of sparse bacterial concentrations are highly susceptible to contamination, false positives, and false negatives. For this reason, the growth and enumeration of bacteria, as well as the preparation of highly dilute samples for DHM are critical steps in this experiment. Caution must be taken to avoid contamination in this experiment by carefully controlling the environment where the bacteria are grown and enumerated. Proper sterilization techniques, including autoclaving, help prevent against contamination as well as false positives. To further prevent against false positives, bacteria were selected for this experiment that exhibit relatively unique characteristics (*e.g., S. marcescens* has a very distinct red color when cultured). To prevent against false negatives, the bacteria chosen for this experiment were selected such that they would be able to grow on enriched culture plates, as well as have characteristic shapes and/or motility patterns to be identified via DHM. It is important to periodically test for contamination and/or unexpected cell growth by plating the samples and quantifying the bacteria by plate count.

In conducting this experiment, a data size of roughly 2.4 GB per 1 mL of sample is expected. This number, of course, is dependent on the camera and file format used. The data size reported is by the use of a 4 Mpx detector and a standard TIFF file format. The post-processing of the data requires roughly 6 min of computation per 1 mL of sample. This processing time was observed while using an Intel i7 8-core processor at 3.5 GHz and 32 GB of RAM. These calculations can be parallelized to the GPU for greatly reduced processing times, but was not done here.

Limitations of the technique

While using DHM to detect very low concentrations of bacteria is possible, this method is non-specific. Morphology alone is not a conclusive means of identifying bacterial strains. Diagnostic applications will present specific challenges due to the presence of non-target cells and aggregates. However, the advantage of the dual-beam instrument presented here is that it is able to image bacteria in relatively turbid samples. The ability to detect bacteria in clinical samples, and the degree of pre-processing of the samples that is required, remain to be determined.

Critical steps in the protocol
Step 2: Obtaining accurate dilutions is essential to quantitative enumeration. Any dilutions made should be backed up by plate count. **Step 3**: The choice of flow rate and corresponding frame rate must be made carefully to ensure that all cells are seen. Adjustment of the pump parameters should be carefully tuned before performing a limit of detection experiment. **Step 4**: For very low bacterial concentrations, it is crucial to capture enough data to be confident of detection. It may be necessary to reconstruct some data to be certain that cells, and not debris, are being seen. In extreme cases, more than 10 mL of solution may be required. Non-motile strains are more likely to be ambiguous than motile strains. **Step 5**: If there is any ambiguity in the data, reconstruction can help demonstrate that holograms represent cells and not debris. High-resolution reconstructions will show classic cell morphologies, and motility can clearly be seen in tracks of motile strains.

Disclosures

The authors have nothing to disclose.

Acknowledgements

The authors acknowledge the Gordon and Betty Moore Foundation Grants 4037 and 4038 to the California Institute of Technology for funding this work.

References

1. Akineden, O., Weirich, S., Abdulmawjood, A., Failing, K., & Buelte, M. Application of a Fluorescence Microscopy Technique for Detecting Viable Mycobacterium avium ssp. paratuberculosis Cells in Milk. *Food Anal. Methods.* **8**, 499-506 (2015).
2. Deibl, J., Paulsen, P., & Bauer, F. Rapid enumeration of total aerobic microbial counts on meat and in meat products by means of the direct epifluorescence filter technique. *Wien Tierarztl Monat.* **85**, 327-333 (1998).
3. Huang, J., Li, Y., Slavik, M. F., Tao, Y., & Huff, G. R. Identification and enumeration of Salmonella on sample slides of poultry carcass wash water using image analysis with fluorescent microscopy. *Transactions of the Asae.* **42**, 267-273 (1999).
4. Durtschi, J. D. *et al.* Increased sensitivity of bacterial detection in cerebrospinal fluid by fluorescent staining on low-fluorescence membrane filters. *J Med Microbiol.* **54**, 843-850 (2005).
5. Panicker, R. O., Soman, B., Saini, G., & Rajan, J. A Review of Automatic Methods Based on Image Processing Techniques for Tuberculosis Detection from Microscopic Sputum Smear Images. *J Med Syst.* **40** (2016).
6. Riepl, M. *et al.* Applicability of solid-phase cytometry and epifluorescence microscopy for rapid assessment of the microbiological quality of dialysis water. *Nephrol Dial Transplant.* **26**, 3640-3645 (2011).
7. Hwang, C. Y., & Cho, B. C. Virus-infected bacteria in oligotrophic open waters of the East Sea, Korea. *Aquat Microb Ecol.* **30**, 1-9 (2002).
8. Kepner, R. L., & Pratt, J. R. Use of Fluorochromes for Direct Enumeration of Total Bacteria in Environmental-Samples - Past and Present. *Microbiol Rev.* **58**, 603-615 (1994).
9. Queric, N. V., Soltwedel, T., & Arntz, W. E. Application of a rapid direct viable count method to deep-sea sediment bacteria. *J Microbiol Meth.* **57**, 351-367 (2004).
10. Prieto-Ballesteros, O., Vorobyova, E., Parro, V., Rodriguez Manfredi, J. A., & Gomez, F. Strategies for detection of putative life on Europa. *Adv Space Res.* **48**, 678-688 (2011).
11. Gleeson, D. F. *et al.* Biosignature Detection at an Arctic Analog to Europa. *Astrobiology.* **12**, 135-150 (2012).
12. Carr, C. E., Zuber, M. T., Ruvkun, G., & Ieee. in *2013 Ieee Aerospace ConferenceIEEE Aerospace Conference Proceedings.* (2013).
13. Konstantinidis, K. *et al.* A lander mission to probe subglacial water on Saturn's moon Enceladus for life. *Acta Astronautica.* **106**, 63-89 (2015).
14. McKay, C. P., Anbar, A. D., Porco, C., & Tsou, P. Follow the Plume: The Habitability of Enceladus. *Astrobiology.* **14**, 352-355 (2014).
15. Hoover, R. B. in *Instruments, Methods, and Missions for Astrobiology Xvii* Vol. 9606 *Proceedings of SPIE.* eds R. B. Hoover, G. V. Levin, A. Y. Rozanov, & N. C. Wickramasinghe) (2015).
16. Handelsman, J. Metagenomics: application of genomics to uncultured microorganisms. *Microbiol Mol Biol Rev: MMBR.* **68**, 669-685 (2004).
17. Lebaron, P., Parthuisot, N., & Catala, P. Comparison of blue nucleic acid dyes for flow cytometric enumeration of bacteria in aquatic systems. *Appl Environ Microbiol.* **64**, 1725-1730 (1998).
18. Marie, D., Partensky, F., Jacquet, S., & Vaulot, D. Enumeration and cell cycle analysis of natural populations of marine picoplankton by flow cytometry using the nucleic acid stain SYBR Green I. *Appl Environ Microbiol.* **63**, 186-193 (1997).
19. Noble, R. T., & Fuhrman, J. A. Use of SYBR Green I for rapid epifluorescence counts of marine viruses and bacteria. *Aquat Microb Ecol.* **14**, 113-118 (1998).
20. Forster, S., Snape, J. R., Lappin-Scott, H. M., & Porter, J. Simultaneous fluorescent gram staining and activity assessment of activated sludge bacteria. *Appl Environ Microbiol.* **68**, 4772-4779 (2002).
21. Lauer, B. A., Reller, L. B., & Mirrett, S. Comparison Of Acridine-Orange And Gram Stains For Detection Of Microorganisms In Cerebrospinal-Fluid And Other Clinical Specimens. *J Clin Microbiol.* **14**, 201-205 (1981).
22. Mason, D. J., Shanmuganathan, S., Mortimer, F. C., & Gant, V. A. A fluorescent gram stain for flow cytometry and epifluorescence microscopy. *Appl Environ Microbiol.* **64**, 2681-2685 (1998).
23. Saida, H., Ytow, N., & Seki, H. Photometric application of the Gram stain method to characterize natural bacterial populations in aquatic environments. *Appl Environ Microbiol.* **64**, 742-747 (1998).
24. Sizemore, R. K., Caldwell, J. J., & Kendrick, A. S. Alternate Gram Staining Technique Using A Fluorescent Lectin. *Appl Environ Microbiol.* **56**, 2245-2247 (1990).

25. Bitton, G., Dutton, R. J., & Foran, J. A. New Rapid Technique For Counting Microorganisms Directly On Membrane Filters. *Stain Technology.* **58**, 343-346 (1983).
26. Broadaway, S. C., Barton, S. A., & Pyle, B. H. Rapid staining and enumeration of small numbers of total bacteria in water by solid-phase laser cytometry. *Appl Environ Microbiol.* **69**, 4272-4273 (2003).
27. Yagupsky, P., & Nolte, F. S. Quantitative aspects of septicemia. *Clin Microbiol Rev.* **3**, 269-279 (1990).
28. Kang, D. K. *et al.* Rapid detection of single bacteria in unprocessed blood using Integrated Comprehensive Droplet Digital Detection. *Nat Commun.* **5**, 5427 (2014).
29. Hand, K. P. *Report of the Europa Lander Science Definition Team.* (2017).
30. Popescu, G. *et al.* Optical imaging of cell mass and growth dynamics. *Am J Physiol-Cell Physiol.* **295**, C538-C544 (2008).
31. Mir, M. *et al.* Optical measurement of cycle-dependent cell growth. *Proc Natl Acad Sci U S A.* **108**, 13124-13129 (2011).
32. Rappaz, B. *et al.* Noninvasive characterization of the fission yeast cell cycle by monitoring dry mass with digital holographic microscopy. *J.Biomed Opt.* **14**, 034049 (2009).
33. Jo, Y. *et al.* Label-free identification of individual bacteria using Fourier transform light scattering. *Opt. Express.* **23**, 15792-15805 (2015).
34. Wallace, J. K. *et al.* Robust, compact implementation of an off-axis digital holographic microscope. *Opt. Express.* **23**, 17367-17378 (2015).
35. Lindensmith, C. A. *et al.* A Submersible, Off-Axis Holographic Microscope for Detection of Microbial Motility and Morphology in Aqueous and Icy Environments. *Plos One.* **11** e0147700 (2016).
36. Dumas, E. M., Ozenne, V., Mielke, R. E., & Nadeau, J. L. Toxicity of CdTe Quantum Dots in Bacterial Strains. *IEEE Trans. NanoBiosci.* **8**, 58-64 (2009).
37. Frisk, A., Jyot, J., Arora, S. K., & Ramphal, R. Identification and functional characterization of flgM, a gene encoding the anti-sigma 28 factor in Pseudomonas aeruginosa. *J Bacteriol.* **184**, 1514-1521 (2002).
38. Adler, J., & Templeton, B. The effect of environmental conditions on the motility of Escherichia coli. *Journal Gen Microbiol.* **46**, 175-184 (1967).
39. Piedrahita-Quintero, P., Castaneda, R., & Garcia-Sucerquia, J. Numerical wave propagation in Image *J. Appl Opt.* **54**, 6410-6415 (2015).
40. Schnars, U., & Jüptner, W. P. Digital recording and numerical reconstruction of holograms. *Meas. Sci. Technol.* **13**, R85 (2002).

